# Hybrid CIGS-Cobalt Quaterpyridine Photocathode with Backside Illumination: a New Paradigm for Solar Fuel Production

Hichem Ichou, Léo Choubrac, Garen Suna, Debashrita Sarkar, Paulo Jorge Marques Cordeiro Junior, Stéphane Diring, Fabien Pineau, Julien J Bonin, Nicolas Barreau, Marc Robert, et al.

How to cite: Angew. Chem. Int. Ed. 2025, e202423727
doi.org/10.1002/anie.202423727

Photoelectrochemical Devices

# Hybrid CIGS-Cobalt Quaterpyridine Photocathode with Backside Illumination: A New Paradigm for Solar Fuel Production

*Hichem Ichou[+], Léo Choubrac[+], Garen Suna[+], Debashrita Sarkar, Paulo Jorge Marques Cordeiro Junior, Stéphane Diring, Fabien Pineau, Julien Bonin, Nicolas Barreau,* Marc Robert,* and Fabrice Odobel**

**Abstract:** Chalcogenide-based thin-film solar cell optimized for rear illumination and used for $CO_2$ reduction is presented. Central to this innovation is a thinner, $Cu(In,Ga)S_2$ chalcopyrite absorber coated with a robust metallic top layer, which potentially surpasses the performance of conventional front-illuminated designs. Using cobalt quaterpyridine molecular catalyst, photocurrent densities for $CO_2$ reduction exceeding 10 mA/cm$^2$ at 0.0 V vs. RHE under 1 Sun illumination, and ca. 16 mA/cm$^2$ at −0.25 V vs. RHE were achieved in voltammetry experiments. Controlled potential electrolysis showed catalytic activity over 20 h with selectivity for CO ranging from >92 % (first 4 hours) to 86 % at the end of the experiment. This approach opens limitless possibilities for employing various reduction catalysts, extending far beyond $CO_2$ reduction. It imposes minimal constraints on absorption properties, immobilization methods, and catalyst nature, setting the stage for high-performance, adaptable PEC devices.

Artificial photosynthesis is both a strategic challenge and a powerful opportunity for advancing sustainable development, as it represents a crucial approach for achieving carbon neutrality across the energy, industrial and transportation sectors. In this context, the integration of efficient and highly selective molecular catalysts on high performance semiconducting photoelectrodes, leading to the development of hybrid solar photoelectrochemical cells (PECs), has recently emerged as a promising and relevant approach for artificial photosynthesis.[1] Despite the progress in this field, there are still numerous obstacles to overcome to build up efficient devices. On the one hand, inorganic semiconductors (SCs) such as silicon, cadmium telluride, chalcopyrite $Cu(In,Ga)(S,Se)_2$ (CIGSSe) and hybrid organic-inorganic perovskites are highly efficient materials for photovoltaic applications, effectively converting photons into electricity.[2] However, they often exhibit limited stability over time especially when in contact with aqueous environments. Homogeneous molecular catalysts are ideal candidates to achieve a high selectivity at low overpotentials[3] and their reactivity can be both studied in details and finely-tuned. Nevertheless, their recycling and achieving efficient charge extraction after immobilization on photoelectrodes remain challenging. In addition, the majority of photoelectrodes are illuminated from the photoactive semiconductor side due to the typical presence of an optically opaque metal layer on the so-called rear contact.[4] This presents a major constraint, as all components topping the photoactive material – including protective materials, buffer layers, and active catalysts- must be transparent to sunlight. Of particular concern is the strong light absorption of several efficient molecular catalysts within the visible range, such as metal porphyrins or metal phthalocyanines.[5] An interesting solution to this problem has recently been proposed by Li and co-workers.[6] It consists of drilling small holes in a strongly absorbing catalytic layer deposited on a $TiO_2$–protected silicon photocathode to let the light reaching the silicon layer upon front side illumination. A similar method has been employed in transparent photovoltaics to fabricate see-through photovoltaic solar cells.[7] However, this strategy does not allow the full exploitation of the SC photoactive

[*] Dr. H. Ichou,[+] Dr. G. Suna,[+] Dr. S. Diring, Dr. F. Odobel
Nantes Université, CNRS, CEISAM, UMR 6230, F-44000 Nantes, France
E-mail: fabrice.odobel@univ-nantes.fr

Dr. L. Choubrac,[+] F. Pineau, Prof. Dr. N. Barreau
Nantes Université, CNRS, Institut des Matériaux de Nantes Jean Rouxel, IMN, F-44000 Nantes, France
E-mail: nicolas.barreau@cnrs-imn.fr

Dr. G. Suna[+]
Present address: Istanbul University, Department of Chemistry, 34134 Istanbul, Turkey

D. Sarkar, Dr. P. J. Marques Cordeiro Junior, Prof. Dr. J. Bonin, Prof. Dr. M. Robert
Université Paris Cité, CNRS, Laboratoire d'Electrochimie Moléculaire (LEM), F-75013 Paris, France
and
Sorbonne Université, CNRS, Institut Parisien de Chimie Moléculaire (IPCM), F-75005 Paris, France

Prof. Dr. M. Robert
Institut Universitaire de France (IUF), F-75005, Paris, France
E-mail: marc.robert@sorbonne-universite.fr

[+] These authors contributed equally to this work

surface, as there is a trade-off between the transmittance of the light to the photoactive layer and the overall efficiency of the cell. Under 1 Sun illumination (AM 1.5G, 100 mW/cm$^2$), the photocathode developed by Li and co-workers only delivered a photocurrent density of 1.5 mA/cm$^2$ at −0.11 V vs. RHE (−0.75 V vs. SCE) for 2 hours in carbonate buffer at pH = 6.8. Furthermore, a protective layer is typically deposited on the SC surface to address the common issue of photocorrosion. $TiO_2$ is the typical material employed for this purpose. However, its suitability for prolonged operational use remains far from being satisfactory.[8] Therefore, preventing direct contact between the electrolyte and the SC with a robust material would be a significant improvement. CIGSSe semiconductors, with their adjustable band gap and their high absorption coefficient, are one of the leading technologies in photovoltaic solar energy conversion, with efficiency reaching 23.6 %.[9] Recent developments also make it one of the most promising choices for photoelectrochemical applications such as $CO_2$ reduction, as recent efforts have shown promising Faradaic efficiencies at low bias potentials.[5a,10] Nevertheless, these results were achieved using a photocathode having the standard structure of CIGSSe-based solar cell, namely with an opaque back contact made of molybdenum. This structure, dedicated to front side illumination, is not adapted to backside illuminated PEC. Very importantly, and in contrary to crystalline silicon which is the predominant SC used in PEC devices,[11] the conduction band (CB) of these copper chalcogenides is very negative (between −0.8 V to −2.0 V vs. SCE depending on the composition).[12] This feature enables the activation of a wide array of catalysts, thereby highlighting their extensive applicability across various reduction reactions. In this vein, we have reported the integration of a molecular catalyst on light-absorbing photocathodes demonstrating the high potential of CIGS for the development of solar-driven hybrid photoelectrodes for $CO_2$ reduction.[13] In one example, the encapsulation of a cobalt phthalocyanine catalyst into a transparent and conductive ZnO nanoporous front layer of a CIGSe solar cell enables to reach a photocurrent around 7 mA/cm$^2$ and 92 % selectivity for $CO_2$ reduction to CO *albeit* in organic medium and at very negative potential bias ($E_{app}$ = −1.7 V vs. SCE).[10a]

The present study investigates an innovative design approach for creating new PEC systems. Specifically, by harnessing backside illumination of the CIGS-based photocathode, high $CO_2$-to-CO PEC conversions were achieved, overcoming the limitations associated with front side illumination (Figure 1). Notably, our approach bypasses the need for transparency in upper layers, including catalysts, and facilitates the separation of the photoelectrode from the electrolyte upon using a conductive layer, even a fully opaque material. The cornerstone of our strategy relies on the use of a CIGS photocathode allowing backside illumination thanks to a transparent conductive oxide (TCO) as the back-contact layer. This innovation paves the way for the development of novel PEC devices free from optical constraints on the upper layers. We have used Cobalt quaterpyridine (CoQPy) as molecular catalyst since it is among the most selective and efficient non-noble element electrocatalysts for $CO_2$ reduction.[5b,14] For example, upon immobilization on multi-walled carbon nanotubes (MWCNTs), CoQPy achieved current density up to 19.9 mA/cm$^2$ at only 440 mV overpotential with 99 % selectivity for CO in aqueous carbonate buffer.[15] These results were confirmed in further studies.[16]

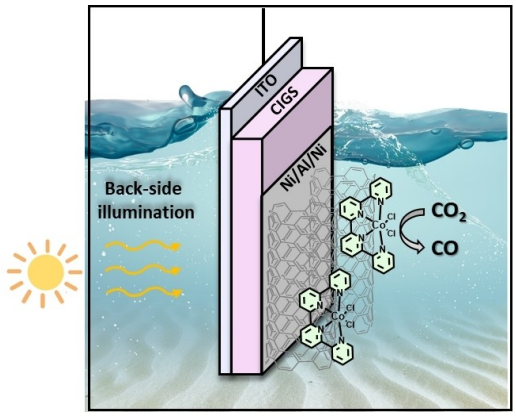


***Figure 1.*** Schematic diagram of the hybrid CIGS photocathode featuring backside illumination.

First, solar cells with the unprecedented structure, compatible with so called backside illumination, were prepared. They consist of 0.5 µm-thick CIGS deposited onto commercially available glass/Indium Tin Oxide (ITO). Details regarding the CIGS growth process can be found in ref.[17] After its completion, the surface of the CIGS layer is completely covered with CdS-buffer, resistive ZnO and Ni/Al/Ni metal stack (Figure 2). Note that compared to the conventional configuration, a significantly thicker resistive ZnO is used, but no ZnO:Al is applied since lateral carrier

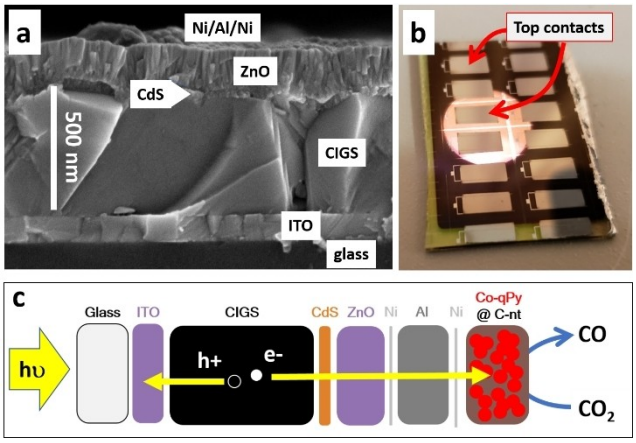


***Figure 2.*** a) Cross-sectional scanning electron microscopy image of the photovoltaic device used in fabricating the PEC; b) Top-view image of the solar cell, highlighting the metallic top contacts. The bright region represents a portion of the sample illuminated from the device's backside; c) Schematic stack diagram of the complete PEC device configuration, illustrating the electron flow to the catalyst, which enhances $CO_2$ reduction.

transport is ensured by the topping metal layer. The resulting device demonstrates outstanding efficiency, above 11 % (Figure S1, Table S1) under rear illumination. A full description of devices preparation and their optoelectronic characteristics are presented in ref.[18]; nonetheless, some of the most important characteristics with respect to PEC application are summarized in the Supplementary Material. The band structure of CIGSSe/CdS/ZnO has been studied several times,[19] demonstrating that the conduction band offset (CBO) at the CIGS/CdS interface should be slightly positive (also called "spike-like") to avoid recombination at this location while the CdS/i-ZnO interface is not a source of limitation. Given its $V_{oc}$ and band gap, the device reported here experiences a 478 mV $V_{oc}$–deficit. This value is similar to state-of-the-art front illuminated CIGS/CdS devices for which interface recombination at the CIGS/CdS interface slightly reduces the $V_{oc}$ but is not strong enough to significantly limit the photocurrent.[17,19a] This has been attributed to an insufficient CBO value (not positive enough, or even slightly negative ("cliff-like")). Using an alternative, higher CB buffer layer material (such as Zn-(O,S)[19a] or $In_xS_y$:Na)[20]) could increase the CBO and thus raise the $V_{oc}$.

These devices are then transformed into PEC as follows. The metal stack completing the solar cell, which shields the semiconductor from electrolyte-induced corrosion and facilitates electron transport, is covered with a drop-casted ink formulated from an ethanolic solution of MWCNTs. The catalyst is finally adsorbed onto the MWCNTs by immersing of the electrode into a CoQPy solution, followed by thorough washing with ethanol and subsequent drying (Figure S2). The prepared photocathode underwent initial characterization using scanning electron microscopy (SEM), with cross-sectional images facilitating comprehensive visualization of the component of each layer (Figure 2).

The highly porous MWCNTs layer, located on the top of the metal layer, displayed a thickness of approximately 10 µm (Figure S3). The catalytic properties of the photoelectrodes were investigated in carbonate buffer (with either Ar or $CO_2$ purging) by cyclic voltammetry (CV) under continuous light irradiation, and then by chopped light linear sweep voltammetry (LSV, Figure 3b). These results have been repeated with minimum three independent photoelectrodes and with two different experimentalists (Figure S4). The active catalyst loading was quantified by assessing the peak current intensity (first reversible reduction wave of the cobalt complex) as a function of the scan rate, yielding a value of $2 \pm 0.3$ nmol/cm$^2$ (Figure S5). Under $CO_2$-saturated carbonate buffer solution, the **CIGS/Ni/Al/Ni/CNT/CoQPy** photoelectrode displays a very early onset potential at about 0.45 V vs. RHE, alongside a remarkable catalytic photocurrent density (Figure 3a, blue) of 10 mA/cm$^2$ at 0.0 V vs. RHE and 16 mA/cm$^2$ at −0.25 V vs. RHE in these short time scale experiments. Control experiments with the same photocathode purged under Ar (Figure 3a) or with a photoelectrode without catalyst (**CIGS/Ni/Al/Ni/CNT**, Figure 3a, top) exhibits negligible photocurrent, due to proton reduction only (see below). These performances are certainly the highest ever reported for solar-driven $CO_2$

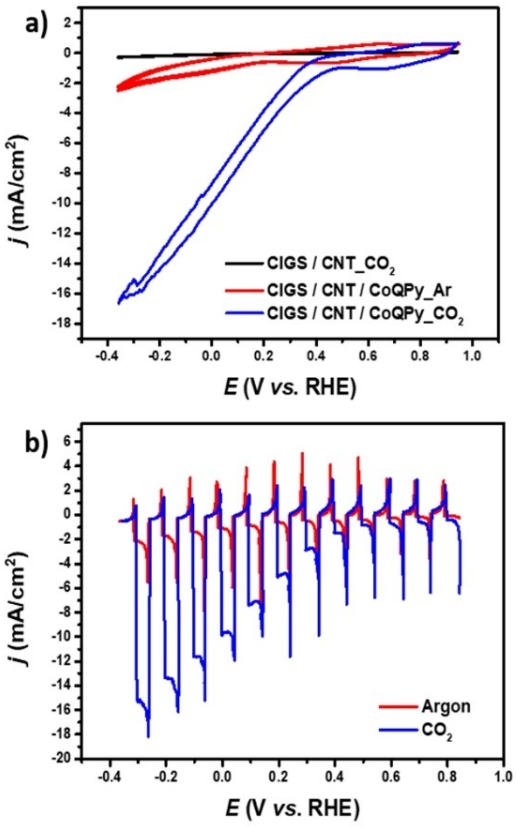


***Figure 3.*** CVs of **CIGS/Ni/Al/Ni/CNT** and **CIGS/Ni/Al/Ni/CNT/CoQPy** under 1 Sun illumination (a). LSV chopped light of **CIGS/Ni/Al/Ni/CNT/CoQPy** under 1 Sun illumination in the presence of argon (red traces) and $CO_2$ (blue traces) (b). Conditions: 0.1 M $KHCO_3$, pH 6.8, Ref.: SCE, CE: Pt mesh. Solar simulator: 100 mW/cm$^2$ AM 1.5G, irradiated surface 0.23 cm$^2$. Scan rate: 30 mV/s for CV and 5 mV/s for LSV.

reduction in aqueous medium with a molecular catalyst, as it displays an apparent positive overpotential of 130 mV relative to the thermodynamic potential of the $CO_2$–to-CO reduction, and a current improvement of more than an order of magnitude as compared to previously published data (Table S2). Compared to dark electrocatalysis using the same CoQPy catalyst deposited on a fluorine-doped tin oxide (FTO) substrate (**FTO/CNT/CoQPy**), that shows an onset potential of ca. −0.5 V vs. RHE, a potential gain of 800 mV is obtained due to solar energy input (Figure S6). This result closely aligns with the photovoltage generated by the photovoltaic cell ($V_{oc} \approx 800$ mV), demonstrating the efficiency of CIGS-based photocathodes and relevance of this novel configuration. Among additional advantages, this configuration facilitates the full utilization of the SC photopotential, since the onset potential is not far from the valence band of CIGS (ca. −0.65 V vs. RHE).[12c]

Control potential electrolysis (CPE) measurements under 1 Sun irradiation were then conducted for 1 h to determine the selectivity, the Faradaic efficiency (FE), the turnover number (TON) and the turnover frequency (TOF) for CO production (Figure 4). At an applied potential of

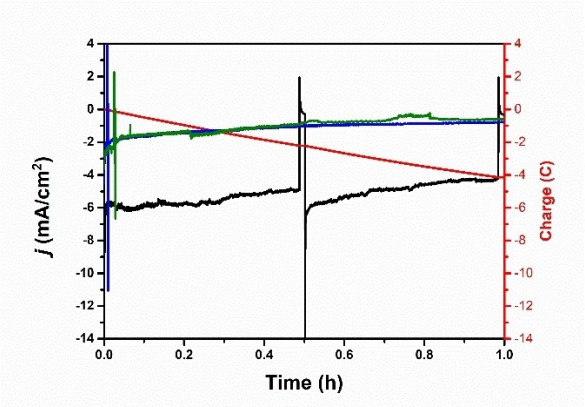


***Figure 4.*** One-hour CPE experiments with **CIGS/NiAlNi/CNT/CoQPy** under $CO_2$ (black); **CIGS/NiAlNi/CNT/CoQPy** under argon (blue) and **CIGS/NiAlNi/CNT** under $CO_2$ (green) Red trace is charge for **CIGS/NiAlNi/CNT/CoQPy** under $CO_2$. $E_{app} = -0.05$ V vs. RHE. 0.1 M $KHCO_3$, pH 6.8, RE: SCE. Pt mesh. Solar simulator 100 mW/cm$^2$, AM 1.5 and a UV 400 nm filter. The surface area of the electrode was 0.23 cm$^2$. The apparent spike in the middle of the experiment is due to short time interruption of light irradiation (few seconds).

−0.05 V vs. RHE, a current density of ca. 6 mA/cm$^2$ was initially obtained in the first 15 min (smaller than in shorter time scale CV), the selectivity for CO was 90 % (remaining 10 % corresponded to $H_2$ formation), with a total FE of 99 %, a TON(CO) in the range of 80,000, and an averaged catalytic rate (TOF(CO)) of ca. 23 s$^{-1}$ (Figure 4). Over one hour of operation, an average partial current density for CO production $j_{CO} = 4.5$ mA/cm$^2$ was thus obtained. These high metrics compare well with electrocatalysis at dark electrode and negative potential,[15] indicating that the catalysis of the photocathode is not limited by the solar cell component of the system. Control experiments conducted with the **CIGS/Ni/Al/Ni/CNT** photocathode, both in the absence of the CoQPy catalyst under a $CO_2$ atmosphere and in the presence of the catalyst but under Ar atmosphere, resulted solely in hydrogen production (Table 1). This underscores the necessity of both $CO_2$ and the catalyst for CO production. Furthermore, the impact of light intensity was assessed by measuring the photocurrent density between 0.3 and 1 Sun at −0.05 V vs. RHE. Notably, a linear correlation was observed, showing that the photocurrent is not limited by catalysis rate (Figure S7). Thus, the efficiency of the system should remain unaffected by fluctuations in the photon flux, presenting a notable advantage, particularly considering the natural variability of sunlight irradiation during daytime and weather conditions. Photoelectrode stability was further investigated by an extensive 20 hours CPE conducted at an applied potential of 0.0 V vs. RHE (Figure S8, Table 2). Remarkably, the selectivity for CO was ca. 92 % in the first four hours and remained as high as 86 % after 20 h of operation with a TON reaching a value of ca. $1.6.10^5$, while the $j_{CO}$ and the catalytic rate for CO production (TOF) experienced progressive lowering over time. From values of 5.6 mA/cm$^2$ and 10.5 s$^{-1}$ after half an hour time of photoelectrolysis, respectively, these two metrics decreased to 0.95 mA/cm$^2$ and 2.2 s$^{-1}$ after 20 h, still with a high selectivity toward CO, $H_2$ remaining a minor by-product (Table 2).

Upon applying a positive bias potential (E = +0.25 V vs. RHE), the current only decreased by ca. 30 % after 14 h of photoelectrocatalysis (Figure S9). CPE experiments were carried out in a continuous flow of $CO_2$, with no observed differences compared to experiments conducted in a standard $CO_2$ atmosphere. Therefore, the decrease in either current over time or selectivity over time cannot be attributed to limited availability of $CO_2$. From previous

***Table 1:*** Performances of one-hour CPE experiments with CIGS/Ni/Al/Ni/CNT/ photoeletrode, with and without CoQPy. $E_{app} = -0.05$ V vs. RHE. 0.1 M $KHCO_3$, pH 6.8, RE: SCE. CE: Pt mesh. Solar simulator 100 mW/cm$^2$, AM 1.5G and a UV 400 nm cutoff filter. Irradiated surface area of the illuminated electrode: 0.23 cm$^2$.

| Photoelectrode | n(CO) (μmol) | n($H_2$) (μmol) | $FE_{TOT}$ (%) | Selectivity CO/$H_2$ (%) | Catalyst loading (nmol/cm$^2$) | TON (CO) | TOF (CO, s$^{-1}$) |
|---|---|---|---|---|---|---|---|
| CIGS/Ni/Al/Ni/CNT_$CO_2$ | 0 | 6.65 ± 0.74 | 99 ± 2.6 | 0/100 | – | 0 | 0 |
| CIGS/Ni/Al/Ni/CNT/CoQPy_Argon | 0 | 3.96 ± 0.38 | 99 ± 1.7 | 0/100 | 0.95 ± 0.4 | 0 | 0 |
| CIGS/Ni/Al/Ni/CNT/ CoQPy_$CO_2$ | 18.1 ± 1.4 | 1.9 ± 0.15 | 99 ± 3.5 | 90 ± 0.5/10 ± 0.5 | 1.16 ± 0.4 | 82 730 ± 2950 | 23 ± 0.8 |

***Table 2:*** Performances of 20 hours CPE experiments with **CIGS/Ni/Al/Ni/CNT/CoQPy**. $E_{app} = 0$ V vs. RHE. 0.1 M $KHCO_3$, pH = 6.8, RE: SCE. CE: Pt mesh. Solar simulator 100 mW/cm$^2$, AM 1.5G and a UV 400 nm cutoff filter. Catalyst loading: 2.3 ± 0.36 nmol/cm$^2$. Irradiated surface area of the illuminated electrode: 0.23 cm$^2$.

| Time | n(CO) (μmol) | n($H_2$) (μmol) | Q (C) | $j_{co}$ (mA/cm$^2$) | Selectivity CO/$H_2$ (%) | $TON_{CO}$ | $TOF_{CO}$ (s$^{-1}$) |
|---|---|---|---|---|---|---|---|
| 0.5 h | 9.7 ± 0.18 | 1.9 ± 0.15 | 2.12 ± 0.16 | 5.1 ± 0.4 | 92 ± 3.5/8 ± 3.5 | 18 400 ± 120 | 10.5 ± 0.1 |
| 1 h | 14.72 ± 0.29 | 1.32 ± 0.14 | 4.14 ± 0.47 | 4.7 ± .0.7 | 92 ± 3.5/8 ± 3.5 | 27 780 ± 250 | 6.3 ± 0.1 |
| 2 h | 31.43 ± 0.86 | 2.07 ± 0.46 | 7.37 ± 0.93 | 3.9 ± 0.7 | 94 ± 3.0/6 ± 3.0 | 59 300 ± 1630 | 8.2 ± 0.45 |
| 4 h | 48.3 ± 9.4 | 4.19 ± 0.5 | 12.0 4 ± 1.82 | 1.9 ± 0.2 | 92 ± 3.5/8 ± 3.5 | 91 210 ± 8230 | 4.3 ± 2.3 |
| 18 h | 77.5 8 ± 3.1 | 11.81 ± 0.86 | 26.68 ± 1.99 | 1.0 ± 0.1 | 87 ± 1.0/13 ± 1.0 | 146 390 ± 5 800 | 2.3 ± 1 |
| 20 h | 84.3 ± 3.6 | 14.14 ± 1.1 | 28.41 ± 2.05 | 0.95 ± 0.1 | 86 ± 1.0/14 ± 1.0 | 159 150 ± 3350 | 2.2 ± 1 |

electrochemical studies,[15] degradation of the catalyst can be ruled out as a major factor. The device stability may thus be contingent on the Ni/Al/Ni/CNT interface stability, and further improvements, such as the incorporation of an additional carbon layer, will be the subject of future investigations aimed at extending long-term durability. Furthermore, we have observed that the degradation of performance is also correlated with the applied external potential. Specifically, when the potential shifts from 0 V vs. RHE to 0.25 V vs. RHE, the stability is markedly enhanced (see Figures S8 and S9).

This study revealed the exceptional potential of back-side-illuminated CIGS photoelectrodes for PEC applications. By designing and fabricating an innovative **CIGS/Ni/Al/Ni/CNT/CoQPy** photocathode, unprecedented photocurrent densities were achieved, reaching 16 mA/cm$^2$ at −0.25 V vs. RHE under one-sun back-side illumination in voltammetry experiments. Remarkably, the solar cell's photovoltage and photocurrent were almost fully converted when operating the photoelectrode under catalytic $CO_2$ reduction conditions. Additionally, the device demonstrated promising stability in long-term experiments. These outstanding PEC performances make this new configuration the most efficient hybrid molecular system immobilized on a photocathode for $CO_2$-to-CO reduction reported to date. Most importantly, this work serves as a pivotal proof of concept for advancing more efficient and stable CIGS-based photocathodes. The versatility of our approach offers boundless opportunities for utilizing diverse reduction catalysts, extending beyond $CO_2$ reduction catalysis, with minimal constraints regarding absorption properties, immobilization mode (covalent or supramolecular interaction), and the nature (molecular, inorganic, COF, or MOF) of the catalyst.

## Supporting Information

Experimental procedures, SEM images, photovoltaic performance data, additional electro- and photo-chemical measurements. The authors have cited additional references within the Supporting Information (Ref. [21,22,23,24,25,26,27,28]).

## Acknowledgements

AMaCC platform's team (CEISAM UMR CNRS 6230, University of Nantes) is gratefully acknowledged for mass spectrometry analytical contributions to this study. This work received financial support from the Region Pays de la Loire with program "trajectoire-nationale" n° 2021 07148, the French National Agency for Research for the project PECALO (ANR-20-CE05-0019-01), the EUR LUMOMAT project (Investments for the Future program ANR-18-EURE-0012) and from the project GreeNH3 (PEPR Hydrogene ANR-22-PEHY-0015). Partial financial support to M.R. from the Institut Universitaire de France (IUF) is also gratefully thanked.

## Conflict of Interest

The authors declare no conflict of interest.

## Data Availability Statement

The data that support the findings of this study are available from the corresponding author upon reasonable request.

**Keywords:** Carbon Dioxide Reduction · Artificial Photosynthesis · Photoelectrochemical Cells · Chalcopyrite

[1] a) D. A. Garcia Osorio, G. Neri, A. J. Cowan, *ChemPhotoChem* **2021**, *5*, 595–610; b) X. Jia, E. Stewart-Jones, J. L. Alvarez-Hernandez, G. P. Bein, J. L. Dempsey, C. L. Donley, N. Hazari, M. N. Houck, M. Li, J. M. Mayer, H. S. Nedzbala, R. E. Powers, *J. Am. Chem. Soc.* **2024**, *146*, 7998–8004; c) V. Andrei, B. Reuillard, E. Reisner, *Nat. Mater.* **2020**, *19*, 189–194; d) J. J. Leung, J. Warnan, K. H. Ly, N. Heidary, D. H. Nam, M. F. Kuehnel, E. Reisner, *Nat. Catal.* **2019**, *2*, 354–365; e) B. Shang, C. L. Rooney, D. J. Gallagher, B. T. Wang, A. Krayev, H. Shema, O. Leitner, N. J. Harmon, L. Xiao, C. Sheehan, S. R. Bottum, E. Gross, J. F. Cahoon, T. E. Mallouk, H. Wang, *Angew. Chem. Int. Ed.* **2023**, *62*, e202215213; f) Z. Wei, Y. Su, W. Pan, J. Shen, R. Fan, W. Yang, Z. Deng, M. Shen, Y. Peng, *Angew. Chem. Int. Ed.* **2023**, *62*, e202305558.

[2] A. Polman, M. Knight, E. Garnett, B. Ehrler, W. Sinke, *Science* **2016**, *352*, aad4424.

[3] S. Ren, D. Joulié, D. Salvatore, K. Torbensen, M. Wang, M. Robert, C. P. Berlinguette, *Science* **2019**, *365*, 367–369.

[4] B. Liu, T. Wang, S. Wang, G. Zhang, D. Zhong, T. Yuan, H. Dong, B. Wu, J. Gong, *Nature Commun.* **2022**, *13*, 7111.

[5] a) E. Boutin, L. Merakeb, B. Ma, B. Boudy, M. Wang, J. Bonin, E. Anxolabéhère-Mallart, M. Robert, *Chem. Soc. Rev.* **2020**, *49*, 5772–5809; b) K. E. Dalle, J. Warnan, J. J. Leung, B. Reuillard, I. S. Karmel, E. Reisner, *Chem. Rev.* **2019**, *119*, 2752–2875.

[6] Z. Wen, S. Xu, Y. Zhu, G. Liu, H. Gao, L. Sun, F. Li, *Angew. Chem. Int. Ed.* **2022**, *61*, e202201086.

[7] C. J. Traverse, R. Pandey, M. C. Barr, R. R. Lunt, *Nat. Energy* **2017**, *2*, 849–860.

[8] D. Bae, B. Seger, P. C. K. Vesborg, O. Hansen, I. Chorkendorff, *Chem. Soc. Rev.* **2017**, *46*, 1933–1954.

[9] J. Keller, K. Kiselman, O. Donzel-Gargand, N. M. Martin, M. Babucci, O. Lundberg, E. Wallin, L. Stolt, M. Edoff, *Nat. Energy* **2024**, *9*, 467–478.

[10] a) J. Guerrero, E. Bajard, N. Schneider, F. Dumoulin, D. Lincot, U. Isci, M. Robert, N. Naghavi, *ACS Energy Lett.* **2023**, *8*, 3488–3493; b) K. Wang, Y. Ma, Y. Liu, W. Qiu, Q. Wang, X. Yang, M. Liu, X. Qiu, W. Li, J. Li, *Green Chem.* **2021**, *23*, 3207–3240; c) Y. Chen, X. Feng, M. Liu, J. Su, S. Shen, *Nanophotonics* **2016**, *5*, 524–547.

[11] a) K. Sun, S. Shen, Y. Liang, P. E. Burrows, S. S. Mao, D. Wang, *Chem. Rev.* **2014**, *114*, 8662–8719; b) D. Zhang, J. Shi, W. Zi, P. Wang, S. Liu, *ChemSusChem* **2017**, *10*, 4324–4341.

[12] a) M. Asaduzzaman, M. Hasan, A. N. Bahar, *SpringerPlus* **2016**, *5*, 578; b) N. Gaillard, D. Prasher, M. Chong, A. Deangelis, K. Horsley, H. A. Ishii, J. P. Bradley, J. Varley, T. Ogitsu, *ACS Applied Energy Mater.* **2019**, *2*, 5515–5524; c) Y. Liu, M. Xia, D. Ren, S. Nussbaum, J.-H. Yum, M. Grätzel, N. Guijarro, K. Sivula, *ACS Energy Lett.* **2023**, *8*, 1645–1651.

[13] P. B. Pati, R. Wang, E. Boutin, S. Diring, S. Jobic, N. Barreau, F. Odobel, M. Robert, *Nature Commun.* **2020**, *11*, 3499.

[14] a) K.-M. Lam, K.-Y. Wong, S.-M. Yang, C.-M. Che, *Dalton Trans.* **1995**, 1103–1107; b) Z. Guo, S. Cheng, C. Cometto, E. Anxolabéhère-Mallart, S.-M. Ng, C.-C. Ko, G. Liu, L. Chen, M. Robert, T.-C. Lau, *J. Am. Chem. Soc.* **2016**, *138*, 9413–9416.
[15] M. Wang, L. Chen, T.-C. Lau, M. Robert, *Angew. Chem. Int. Ed.* **2018**, *57*, 7769–7773.
[16] a) L. Sun, V. Reddu, S. Xi, C. Dai, Y. Sheng, T. Su, A. C. Fisher, X. Wang, *Adv. Energy Mater.* **2022**, *12*, 2202108; b) V. Reddu, L. Sun, X. Li, H. Jin, S. Wang, X. Wang, *SmartMat* **2022**, *3*, 151–162.
[17] L. Choubrac, E. Bertin, F. Pineau, L. Arzel, T. Lepetit, L. Assmann, T. Aloui, S. Harel, N. Barreau, *Prog. Photovolt. Res. Appl.* **2023**, *31*, 971–980.
[18] L. Choubrac, F. Pineau, E. Bertin, L. Arzel, N. Barreau, *JPhys Energy* **2024**, 10.1088/2515-7655/ad9acf.
[19] a) https://orbilu.uni.lu/handle/10993/48952; b) X. Shang, Z. Wang, M. Li, L. Zhang, J. Fang, J. Tai, Y. He, *Thin Solid Films* **2014**, *550*, 649–653; c) M. Rusu, T. Kodalle, L. Choubrac, N. Barreau, C. A. Kaufmann, R. Schlatmann, T. Unold, *ACS Appl. Mater. Interfaces* **2021**, *13*, 7745–7755.
[20] D. Hauschild, F. Meyer, A. Benkert, D. Kreikemeyer-Lorenzo, T. Dalibor, J. Palm, M. Blum, W. Yang, R. G. Wilks, M. Bär, F. Reinert, C. Heske, L. Weinhardt, *Prog. Photovolt. Res. Appl.* **2018**, *26*, 359–366.
[21] C.-F. Leung, S.-M. Ng, C.-C. Ko, W.-L. Man, J. Wu, L. Chen, T.-C. Lau, *Energy Environ. Sci.* **2012**, *5*, 7903–7907.
[22] Z. Hu, J. Gong, Z. Ye, Y. Liu, X. Xiao, J. C. Yu, *J. Catal.* **2020**, *384*, 88–95.
[23] H. Kumagai, G. Sahara, K. Maeda, M. Higashi, R. Abe, O. Ishitani, *Chem. Sci.* **2017**, *8*, 4242–4249.
[24] K. Sekizawa, S. Sato, T. Arai, T. Morikawa, *ACS Catal.* **2018**, *8*, 1405–1416.
[25] A. Aitbekova, N. Watkins, M. H. Richter, P. Jahelka, J. C. Peters, T. Agapie, H. A. Atwater, *Nano Lett.* **2024**, *24*, 1090–1095.
[26] B. Shan, S. Vanka, T.-T. Li, L. Troian-Gautier, M. K. Brennaman, Z. Mi, T. J. Meyer, *Nat. Energy* **2019**, *4*, 290–299.

Manuscript received: December 4, 2024
Revised manuscript received: December 30, 2024
Accepted manuscript online: January 31, 2025
Version of record online: ■■, ■■

# Communication

**Photoelectrochemical Devices**

H. Ichou, L. Choubrac, G. Suna, D. Sarkar, P. J. Marques Cordeiro Junior, S. Diring, F. Pineau, J. Bonin, N. Barreau,* M. Robert,* F. Odobel* **e202423727**

Hybrid CIGS-Cobalt Quaterpyridine Photocathode with Backside Illumination: A New Paradigm for Solar Fuel Production

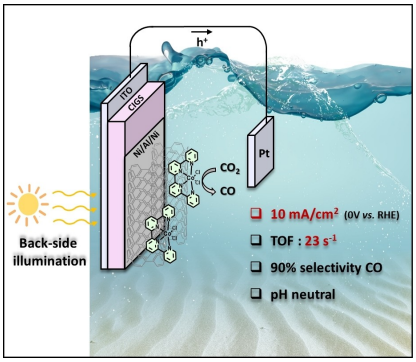


An efficient and selective solar-driven conversion of $CO_2$ to CO has been achieved using a $Cu(In,Ga)S_2$ chalcopyrite-based photocathode, coated with a cobalt molecular catalyst and operated under backside illumination. This innovative design addresses the challenges associated with the absorption properties of the catalyst and the protection layer, paving the way for high-performance and versatile photoelectrochemical (PEC) devices.